nature biotechnology

SUPPLEMENTARY INFORMATION

https://doi.org/10.1038/s41587-019-0335-4

In the format provided by the authors and unedited.

Harnessing the intracellular triacylglycerols for titer improvement of polyketides in *Streptomyces*

Weishan Wang[1,2,10]*, Shanshan Li[3,10], Zilong Li[1,10], Jingyu Zhang[2,10], Keqiang Fan[1], Gaoyi Tan[2], Guomin Ai[1], Sin Man Lam[4], Guanghou Shui[4], Zhiheng Yang[2], Hongzhong Lu[2], Pinjiao Jin[3], Yihong Li[1], Xiangyin Chen[2], Xuekui Xia[5], Xueting Liu[2,6], H. Kathleen Dannelly[7], Chen Yang[8], Yi Yang[2], Siliang Zhang[2], Gil Alterovitz[9], Wensheng Xiang[3]* and Lixin Zhang[2]*

[1]State Key Laboratory of Microbial Resources, Institute of Microbiology, Chinese Academy of Sciences, Beijing, China. [2]State Key Laboratory of Bioreactor Engineering, East China University of Science and Technology, Shanghai, China. [3]State Key Laboratory for Biology of Plant Diseases and Insect Pests, Institute of Plant Protection, Chinese Academy of Agricultural Sciences, Beijing, China. [4]State Key Laboratory of Molecular Developmental Biology, Institute of Genetics and Developmental Biology, Chinese Academy of Sciences, Beijing, China. [5]Key Biosensor Laboratory of Shandong Province, Biology Institute, Qilu University of Technology (Shandong Academy of Sciences), Jinan, China. [6]Laboratory for Marine Biology and Biotechnology, Qingdao National Laboratory for Marine Science and Technology, Qingdao, China. [7]Indiana State University, Terre Haute, IN, USA. [8]CAS-Key Laboratory of Synthetic Biology, CAS Center for Excellence in Molecular Plant Sciences, Shanghai Institute of Plant Physiology and Ecology, Chinese Academy of Sciences, Shanghai, China. [9]Boston Children's Hospital, Boston, MA, USA. [10]These authors contributed equally: Weishan Wang, Shanshan Li, Zilong Li, Jingyu Zhang. *e-mail: wangws@im.ac.cn; xiangwensheng@neau.edu.cn; lxzhang@ecust.edu.cn

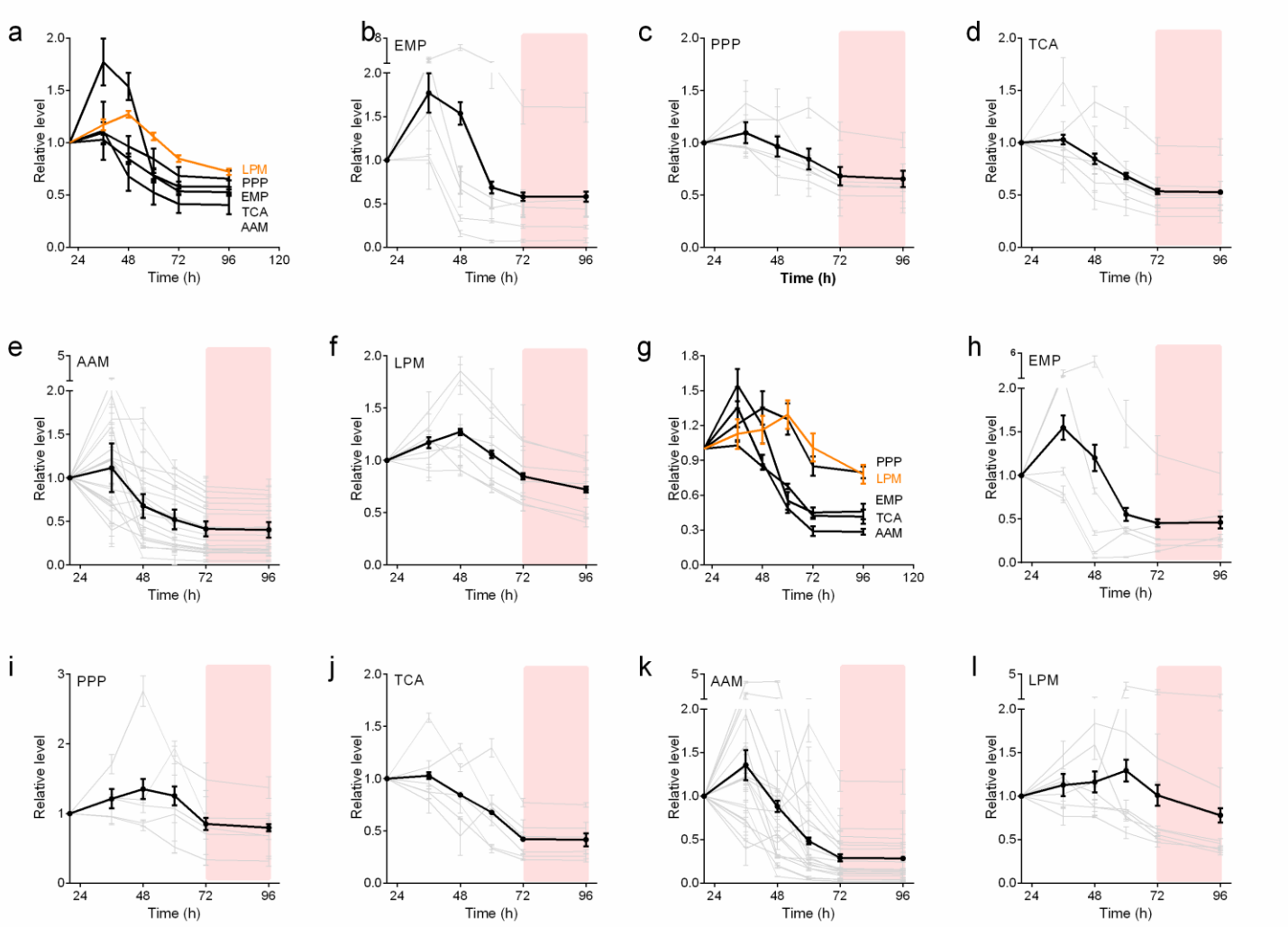

Supplementary Figure 1

Trends of the metabolic pathways in M145 and HY01.

Black bold lines indicate the overall trends of the metabolites involved in the five investigated pathways, and light gray lines show the trends of individual metabolites. Pink background indicates the late stationary phase. (a and g) Overall trends of metabolites in different metabolic pathways in M145 and HY01, respectively. Trend of each metabolite investigated in different pathways were as follows: (b and h) glucose-6-phosphate, dihydroxyacetone phosphate, glyceraldehyde 3-phosphate, D-glycerate 3-phosphate, and pyruvate for glycolysis (EMP) in M145 and HY01, respectively; (c and i) D-altro-heptulose 7-phosphate, D-erythrose 4-phosphate, 6-phospho-D-gluconate, D-ribose, and D-ribulose 5-phosphate for pentose phosphate pathway (PPP) in M145 and HY01, respectively; (d and j) succinic acid, isocitric acid, fumaric acid, citrate, DL-malic acid, and α-ketoglutarate for tricarboxylic acid cycle (TCA) in M145 and HY01, respectively; (e and k) serine, glycine, L-valine, L-threonine, L-pyroglutamic acid, L-proline, L-leucine, L-isoleucine, L-aspartic acid, L-alanine, DL-ornithine, 5-oxo-L-proline, 3-phosphoserine, N-acetyl-L-glutamic acid, and α-ketoadipic acid for amino acid metabolism (AAM) in M145 and HY01, respectively; (f and l) myristic acid, pentadecanoic acid, hexadecanoic acid, margaric acid, octadecanoic acid, MG(16:0/0:0/0:0), and MG(18:0/0:0/0:0) for lipid metabolism (LPM) in M145 and HY01, respectively. Levels of metabolites determined at 20 h were set as one. Data were the average and s.d. of five independent experimental replicates.

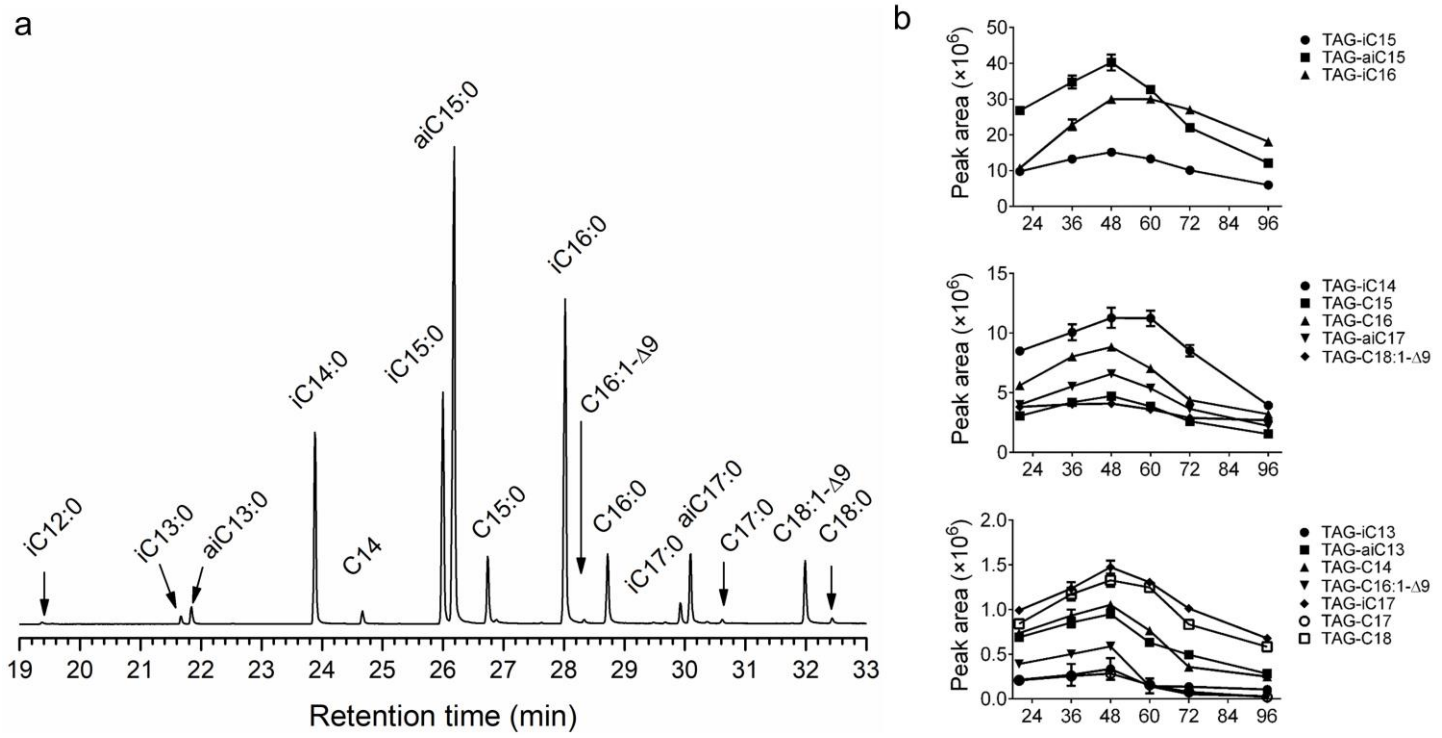

Supplementary Figure 2

Analysis of cellular TAGs by GC-MS.

(a) Fatty acid moieties of cellular TAG pool identified by GC-MS. Fatty acid abbreviations used were as follows: iC12:0, isolauric acid; iC13:0, isotridecanoic acid; aiC13:0, anteisotridecanoic acid; iC14:0, isomyristic acid; C14:0, myristic acid; iC15:0, isopentadecanoic acid ; aiC15:0, anteisopentadecanoic acid ; C15:0, pentadeclic acid; iC16:0, isopalmitic acid; C16:1-Δ9, 9-hexadecenoic acid; C16:0, palmitic acid; iC17:0, isoheptadecanoic acid; aiC17:0, anteisoheptadecanoic acid; C17:0, heptadecanoic acid; C18:1-Δ9, 9-octadecenoic acid; and C18:0, stearic acid. (b) Trends of fatty acid moieties of cellular TAG pool in M145. The cellular TAGs from the time-course samples were firstly hydrolyzed to release fatty acid moieties, and then the fatty acids were quantified using GC-MS. Peak areas of the mass chromatograms were used to indicate the relative levels of the corresponding fatty acid moieties. Results shown are average and s.d. of five independent experimental replicates.

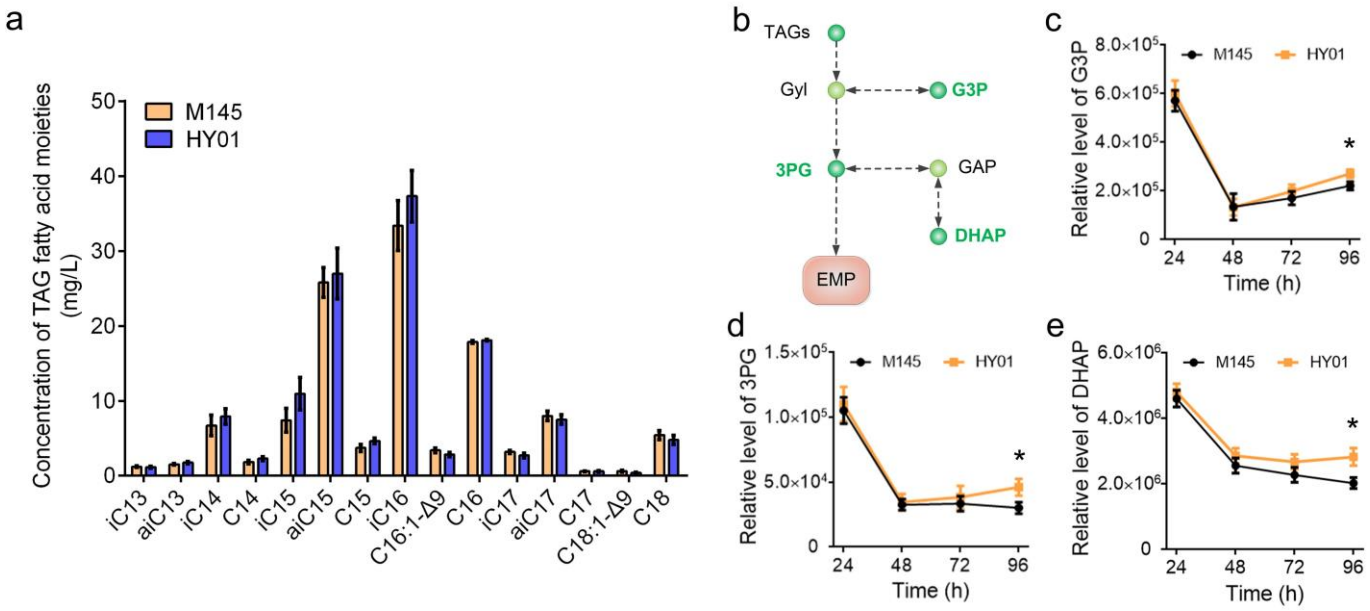

Supplementary Figure 3

Change of cellular TAGs and their derived intermediate metabolite during stationary phase in M145 and HY01.

(a) Levels of TAG pools in M145 and HY01 at transition phase. Columns show the consumed amount of fatty acid moieties from TAGs at 48 h. The level of each fatty acid moiety in M145 and HY01 shows no significant difference (Student *t*-test, $p < 0.05$). (b-e) Levels of the metabolites derived from TAG degradation. (b) Schematic of the metabolic pathway related to TAG degradation. (c-e) Levels of metabolites related to TAG degradation. Metabolite levels are determined by LC-MS/MS. G3P, glycerol-3-phosphate; 3PG, 3-phosphoglycerate; DHAP, dihydroxyacetone phosphate. Data shown are the average and s.d. of three independent experiments. The levels of significance are *** $p < 0.001$, ** $p < 0.01$, * $p < 0.05$.

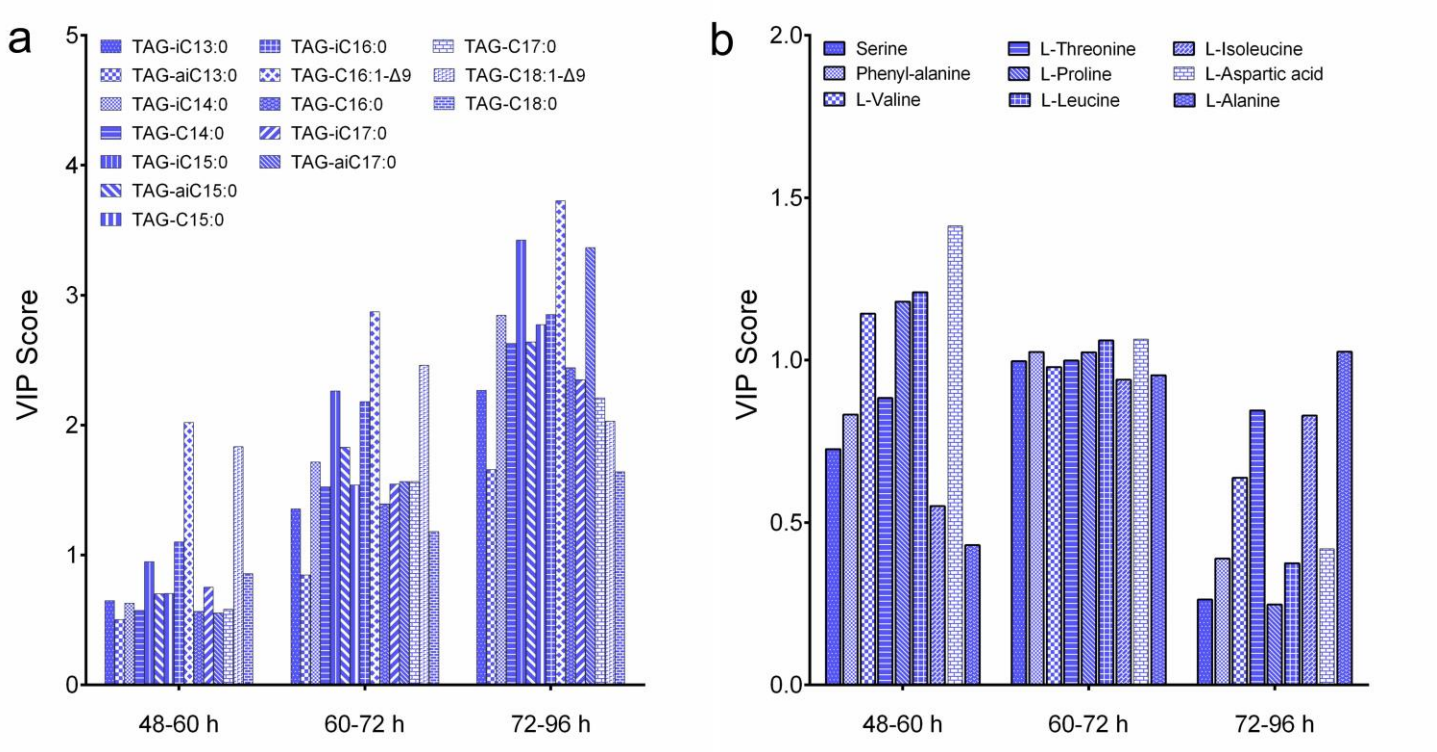

Supplementary Figure 4

Contributions of metabolites on Act production during stationary phase.

(a) Contributions of fatty acid moieties of cellular TAG pool on Act production during stationary phase. (b) Contributions of intercellular amino acids on Act production during stationary phase. VIP score is used to identify important features from the examined samples (Nat. Protoc. 6, 743-760, 2011). Here we aimed to identify important metabolites for Act production using VIP score. VIP score was obtained by comparing the data matrix of M145 and HY01 from different period of stationary phase (48-60 h, 60-72 h, and 72-96 h) using MetaboAnalyst Software.

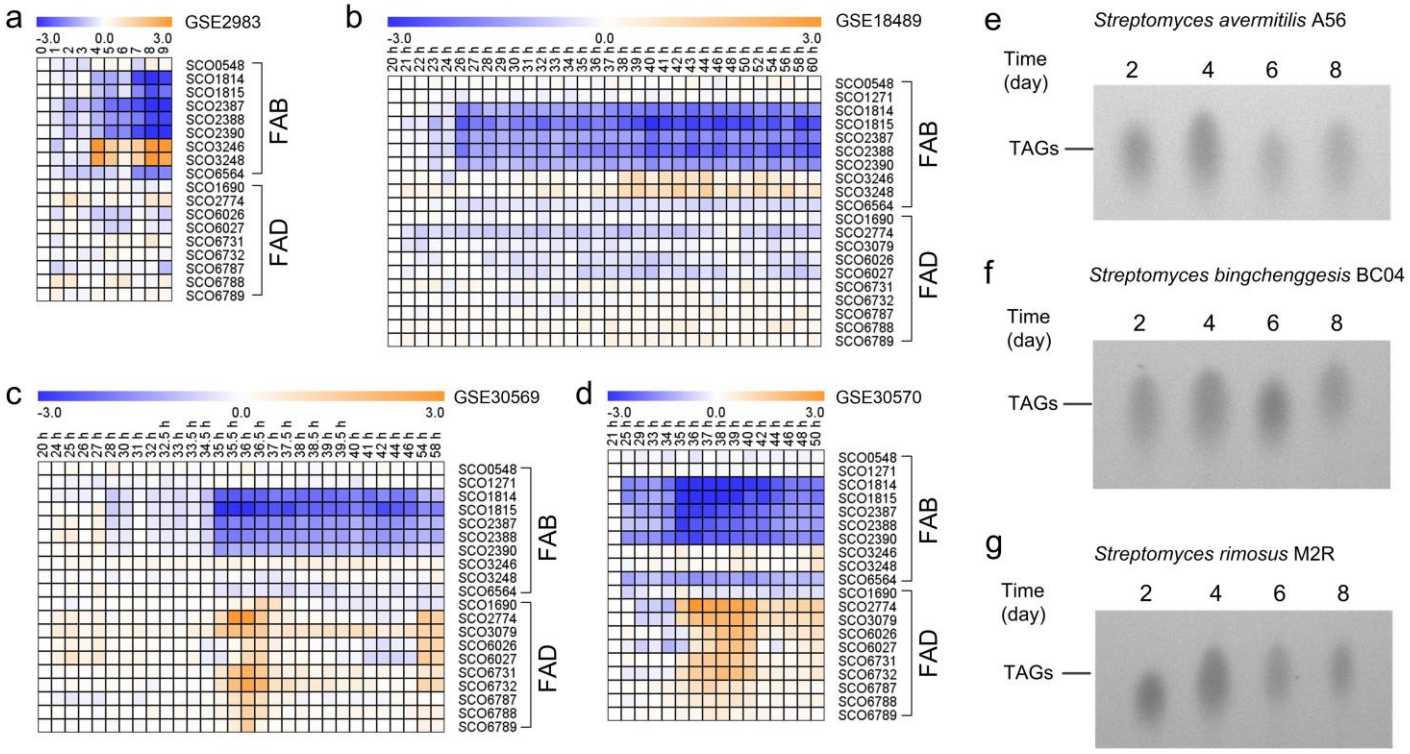

Supplementary Figure 5

Dynamic profile of genes and metabolites related to TAG metabolism.

(a-d) Transcript profiles of the genes in fatty acid metabolism under diverse culture conditions. The selected genes are the same as those shown in Fig. 2e and f. Time-series transcriptome data were obtained from NCBI GEO database: (a) GSE2983, M145 cultivated in modified R5 medium (Genes Dev. 15, 3183-3192, 2001); (b) GSE18489, M145 cultivated in a fermentation medium (BMC Genomics 11, 10, 2010); (c) GSE30569, the *glnK* mutant of M145 cultivated in SSBM-E medium (Appl. Microbiol. Biotechnol. 92, 1219-1236, 2011); (d) GSE30570, M145 cultivated in SSBM-E medium (Appl. Microbiol. Biotechnol. 92, 1219-1236, 2011). (e-g) Profiles of cellular TAG pools in industrial *Streptomyces avermitilis* A56 (Proc. Natl. Acad. Sci. U. S. A. 107, 11250-11254, 2010; Synth. Syst. Biotechnol. 1, 7-16, 2016), *Streptomyces bingchenggesis* BC04 (Microb. Cell Fact. 15, 152, 2016), and *Streptomyces rimosus* M2R (M4018::2SFOtcR) (Microb. Cell Fact. 14, 46, 2015), respectively. The amount of cellular TAG pool was analyzed by TLC.

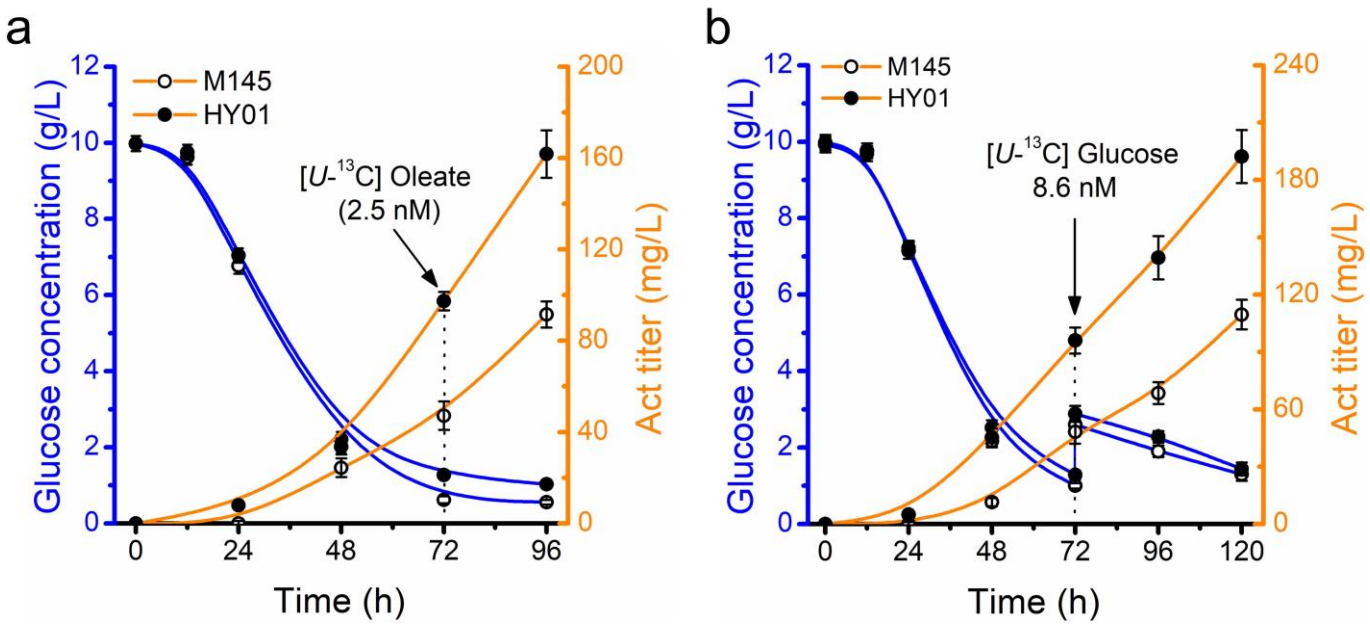

Supplementary Figure 6

Isotopic feeding experiments in M145 and HY01.

(a) Feeding experiments with [*U*-^{13}C] oleate. 2.5 nM [*U*-^{13}C] oleate was added in cultures of M145 and HY01 at 72 h. The samples were harvested after 24 h. (b) Feeding experiments with [*U*-^{13}C] glucose. 8.6 nM [*U*-^{13}C] glucose was added in cultures of M145 and HY01 at 72 h. The samples were harvested after 48 h labeling. Data shown are the average and s.d. of three independent experiments.

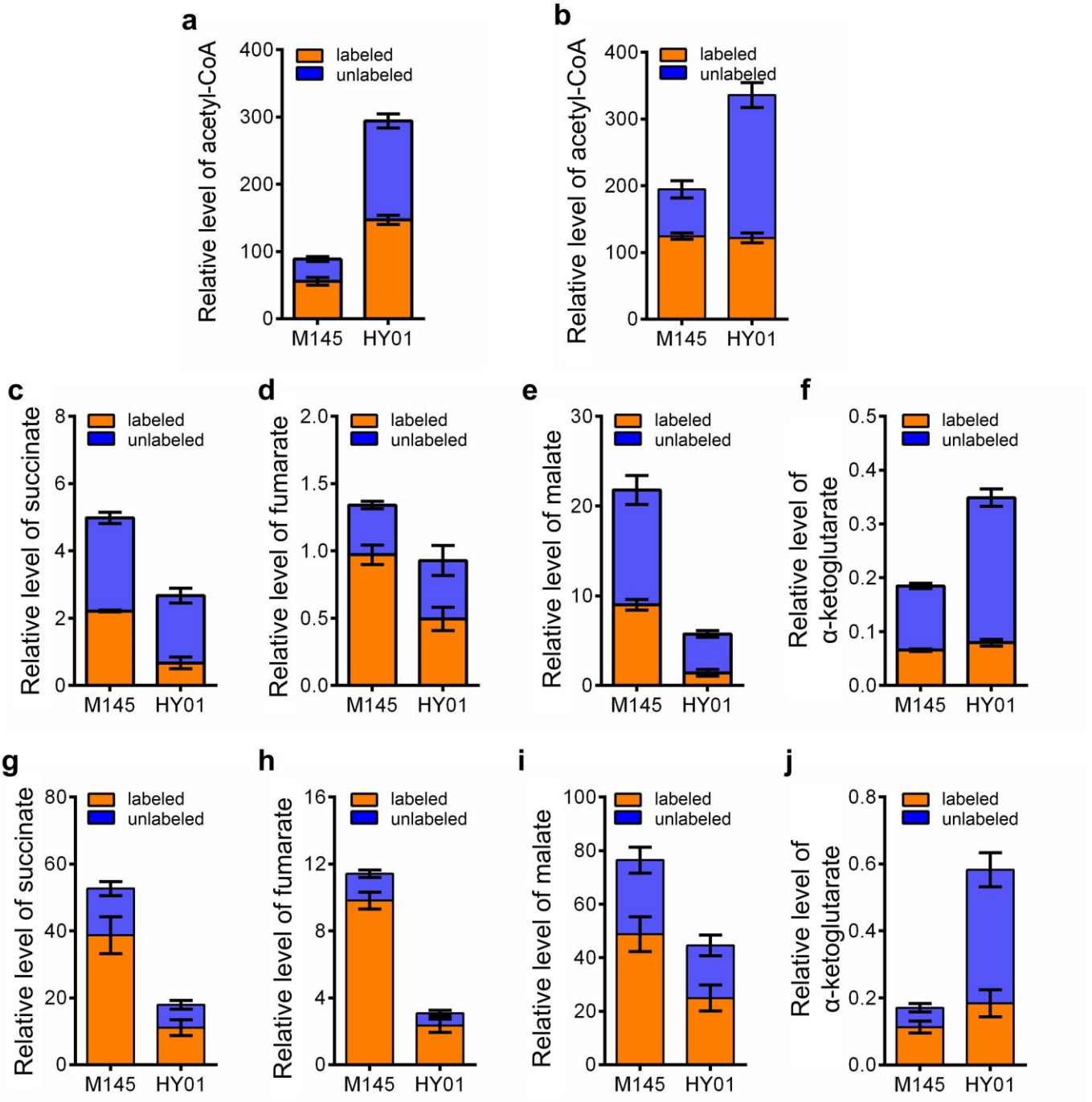

Supplementary Figure 7

Levels of intermediates.

The level is indicated by the peak area of metabolites. (a) Levels of acetyl-CoA obtained from [*U*-^{13}C] oleate feeding experiments. (b) Levels of acetyl-CoA obtained from [*U*-^{13}C] glucose feeding experiments. (c–f) Levels of the TCA intermediates obtained from [*U*-^{13}C] oleate feeding experiments. (g–j) Levels of the TCA intermediates obtained from [*U*-^{13}C] glucose feeding experiments. Data of oleate and glucose labeling experiments were collected at 96 h and 120 h, respectively (Supplementary Fig. 6). Data shown are the average and s.d. of three independent experiments.

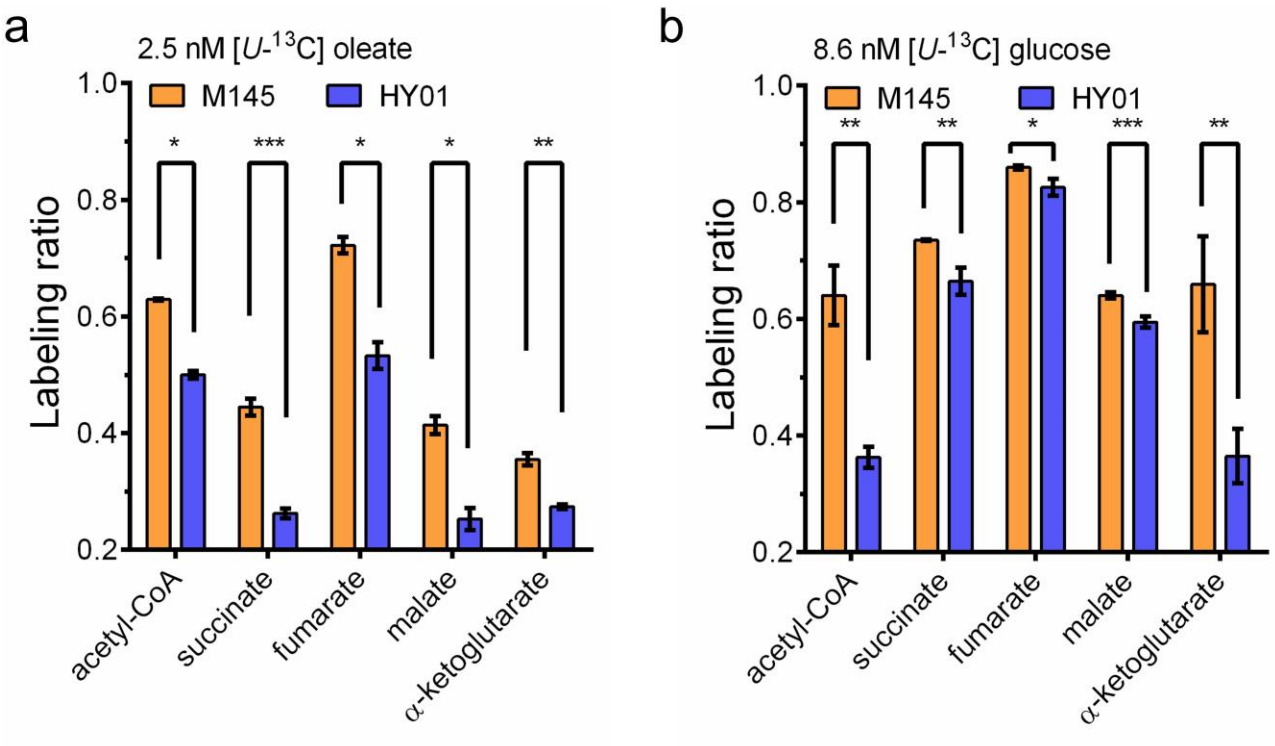

Supplementary Figure 8

Comparison of labeling ratio of TCA intermediates in M145 and HY01.

(a) Labeling ratio obtained from [*U*-^{13}C] oleate feeding experiments. (b) Labeling ratio obtained from [*U*-^{13}C] glucose feeding experiments. The labeling ratio of TCA intermediates in HY01 were normalized with that of the direct input acetyl-CoA using the following equation: normalized labeling ratio = labeling_ratio × (labeling ratio of acetyl-CoA$_{HY01}$ / labeling ratio of acetyl-CoA$_{M145}$). Differences were analyzed by Student *t*-test, and $p < 0.05$ was considered statistically significant. The levels of significance are *** $p < 0.001$, ** $p < 0.01$, * $p < 0.05$. Data shown are the average and s.d. of three independent experiments.

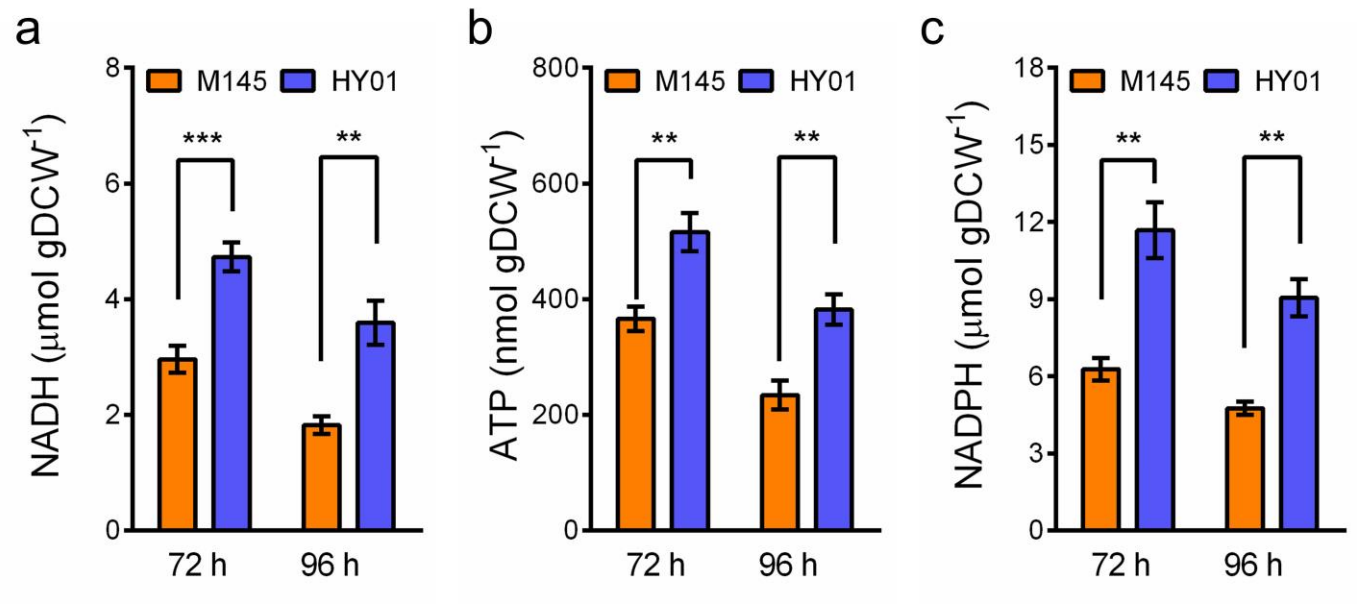

Supplementary Figure 9

Cellular levels of reducing equivalents and ATP.

(a–c) Cellular levels of NADH, ATP and NADPH, respectively, in M145 and HY01 during stationary phase (72, and 96 h). Differences were analyzed by Student *t*-test, and $p < 0.05$ was considered statistically significant. The levels of significance are *** $p < 0.001$, ** $p < 0.01$, * $p < 0.05$. Data shown are the average and s.d. of three independent experiments.

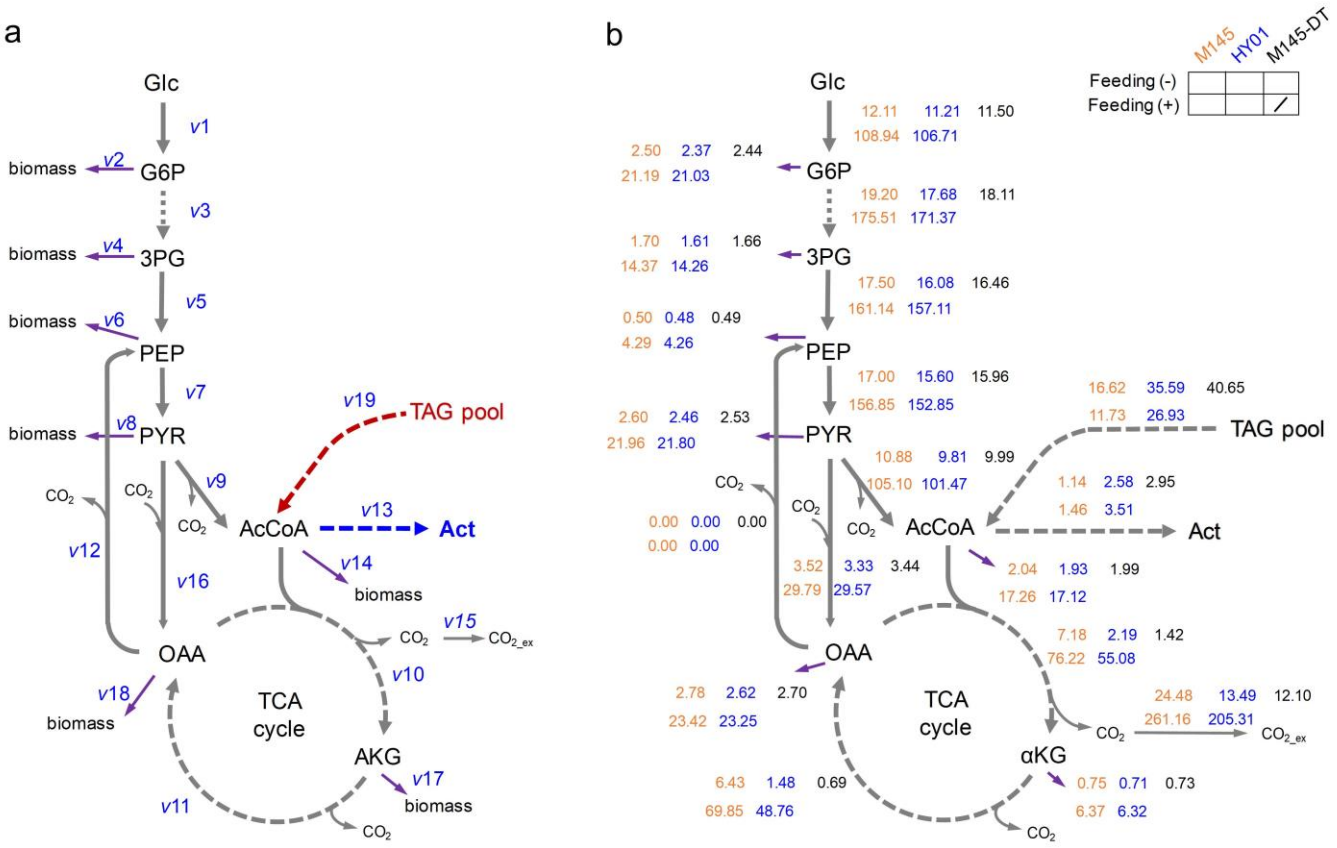

Supplementary Figure 10

Carbon flux distribution of *S. coelicolor* by metabolic flux analysis.

(a) Simplified metabolic network of *S. coelicolor*. Flux for biomass biosynthesis from the G6P node (*v*2) including fluxes from five different precursors (glucose-6-phosphate, fructose-6-phosphate, ribose-5-phosphate, erythrose-4-phosphate, glyceraldehyde-3-phosphate). 15 fatty acid moieties from cellular TAGs are detected in *S. coelicolor*, here flux *v*19 represents the sum of specific production rate of AcCoA from degradation of these fatty acids. The biochemical reactions, stoichiometric equations and experimentally determined fluxes are shown in Supplementary Table 6–8. (b) Actual fluxes of M145, HY01 and M145-DT in fermentation with (+) or without (-) glucose feeding. Data for metabolic flux analysis were collected during stationary phase (72–120 h). Data shown here were the average of three independent experiments. Abbreviations: Glc, glucose; G6P, glucose-6-phosphate; 3PG, 3-phosphate-glycerate; PEP, phosphoenolpyruvate; PYR, pyruvate; AcCoA, acetyl coenzyme A; AKG, alpha-ketoglutaric acid; OAA, oxaloacetic acid; TAG, triacylglycerol; Act, actinorhodin.

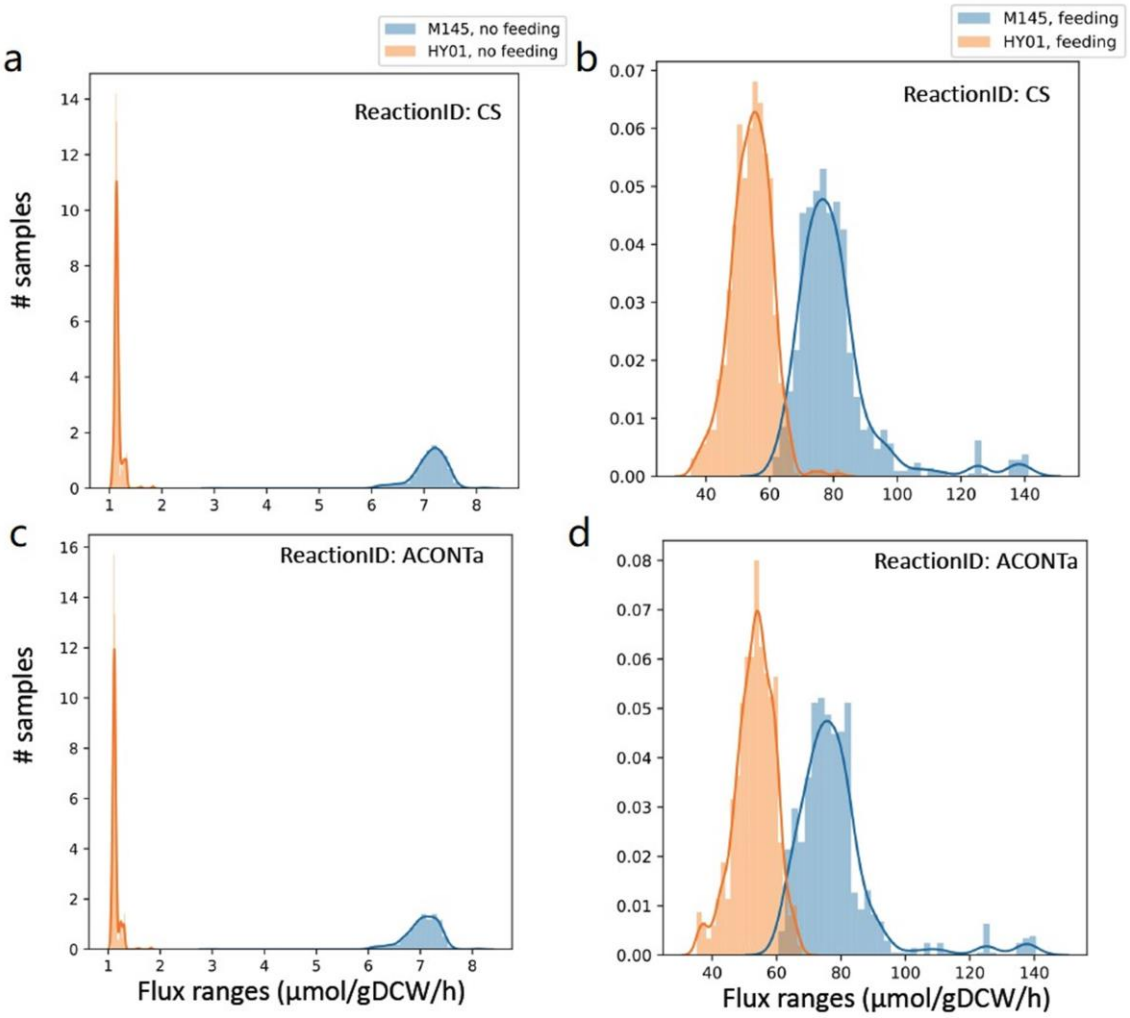

Supplementary Figure 11

Sampling analysis of flux distribution in M145 and HY01.

The genome-scale metabolic model (GEM) of *S. coelicolor* (iKS1317) (Biotechnol. J 14, e1800180, 2019) was constrained by the experimentally measured rate (Supplementary Table 8) with the minimization of glucose uptake rate as the objective function. During the simulation, the sampling algorithm optGpSampler (PLoS One 9, e86587, 2014) was adopted. For each condition, 1000 samples were used for valid sampling distributions. Here we showed two reactions from TCA cycle as examples. (a) Flux changes of reactions catalyzed by citrate synthase (CS) in batch fermentation (without glucose feeding). (b) Flux changes of reactions catalyzed by CS in fed-batch fermentation (with glucose feeding). (c) Flux changes of reactions catalyzed by aconitase (ACONTa) in batch fermentation (without glucose feeding). (d) Flux changes of reactions catalyzed by ACONTa in fed-batch fermentation (with glucose feeding).

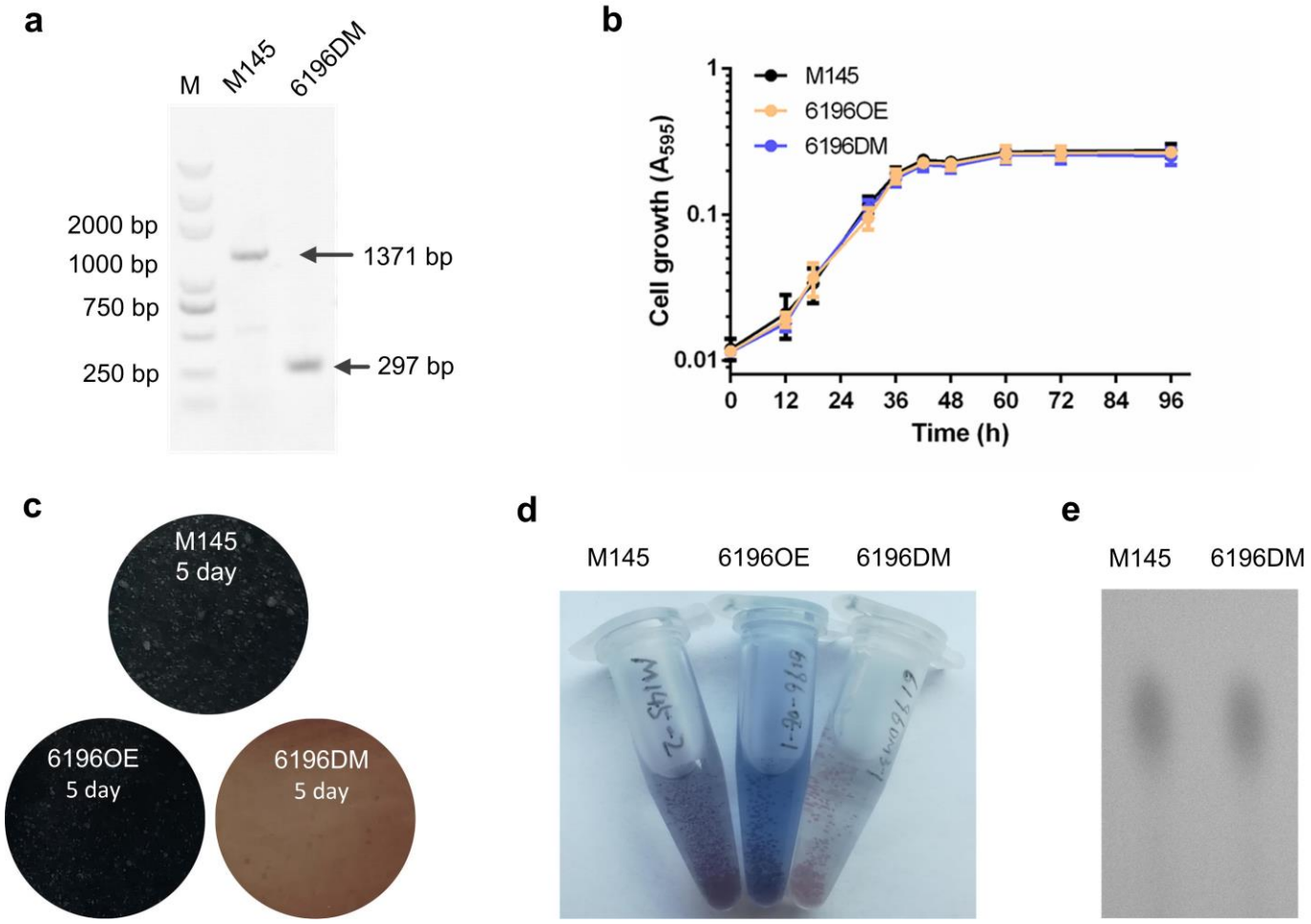

Supplementary Figure 12

Construction of *sco6196* deletion and overexpression strains.

6196DM, *sco6196* deletion strain; 6196OE, *sco6196* overexpression strain. (a) Confirmation of 6196DM.The primer pair 96vF/96vR for PCR amplification is listed in Supplementary table 14. (b) Effect of SCO6196 on cell growth. Data shown here were the average of three independent experiments. (c) Effect of SCO6196 on Act production. The picture shown here was the bottom of the solid plates. (d) Act production of M145, 6196OE and 6196DM in liquid SMM medium. (e) TLC assay of the cellular TAG pools in M145 and 6196DM at transition phase (48 h).

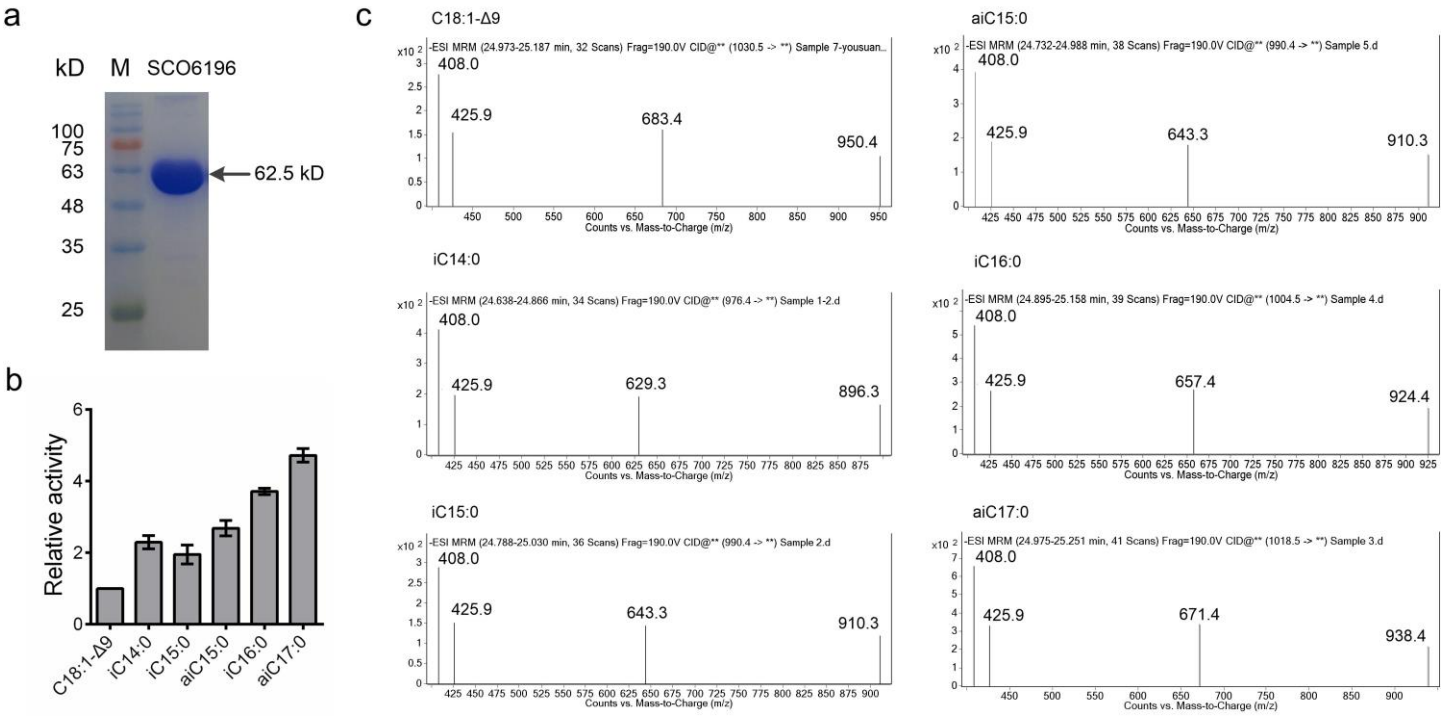

Supplementary Figure 13

Biochemical analysis of substrate specificity of SCO6196 *in vitro*.

(a) SDS-PAGE of the purified recombinant protein SCO6196. (b) Relative activities of SCO6196 when adding different fatty acids. When using C18:1-Δ9 as a substrate, the activity of SCO6196 was set to one. Data shown here were the average of three independent experiments. (c) Specific daughter ions used for the quantification of the corresponding acyl-CoAs from C18:1-Δ9, iC14:0, iC15:0, aiC15:0, iC16:0, aiC17:0, respectively. These daughter ions were selected based on *m/z* 425.9 and 408 in common and specific ions of $[M-H-80]^-$ and $[M-H-347]^-$.

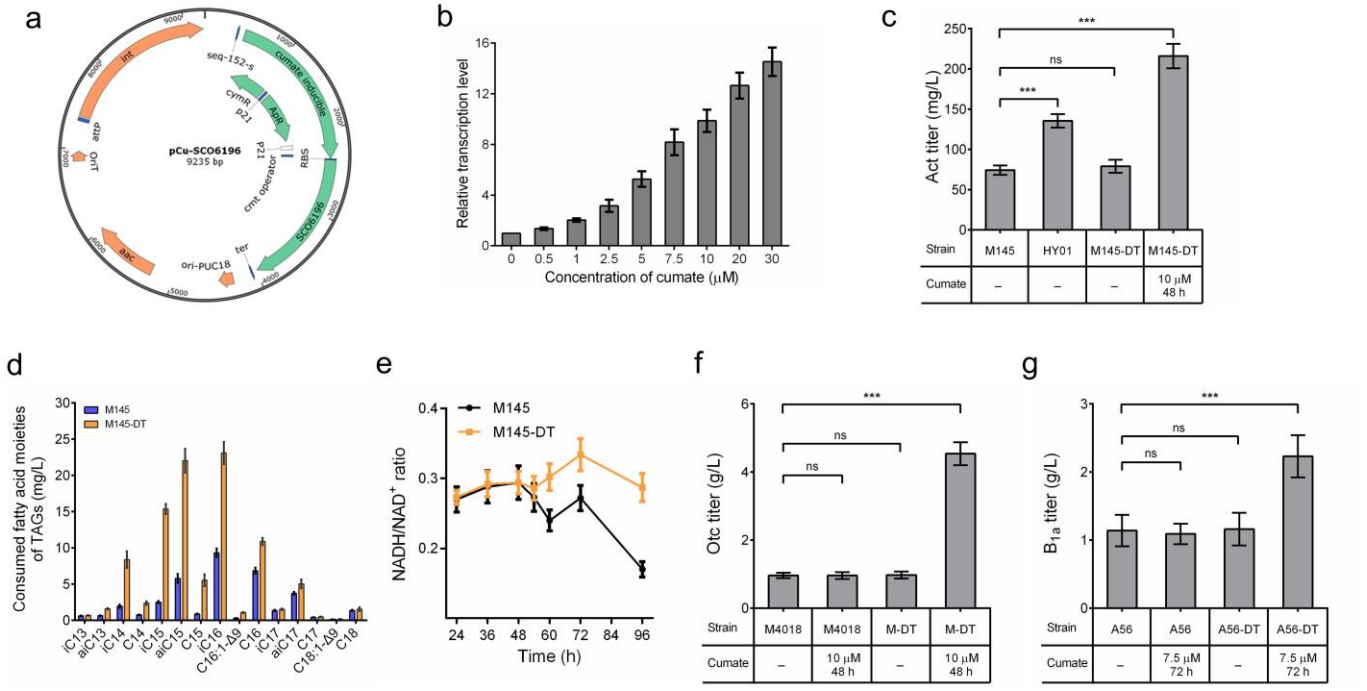

Supplementary Figure 14

Construction and application of the ddTAG module.

(a) Map of the plasmid used to construct the ddTAG module. The ddTAG module is controlled by a cumate inducible system (Appl. Microbiol. Biotechnol. 98, 8641-8655, 2014). (b) Induction range of *sco6196* transcripts quantified by RT-qPCR. (c) Comparison of the Act titers of M145, HY01 and M145-DT. (d) Comparison of the amount of consumed TAGs between M145 and M145-DT. Columns show the consumed amount of fatty acid moieties from cellular TAG pool between 48 h and 96 h. (e) Comparison of the redox status ($NADH/NAD^+$) in M145-DT and M145. (f) Effects of cumate on oxytetracycline (Otc) titer of M4018 and M-DT. (f) Effects of cumate on B_{1a} titer of A56 and A56-DT. Data shown in (b-g) are the average and s.d. of three independent experiments. Significant differences were analyzed by one-way ANOVA, and $p < 0.05$ was considered statistically significant. The levels of significance are *** $p < 0.001$, ** $p < 0.01$, * $p < 0.05$.

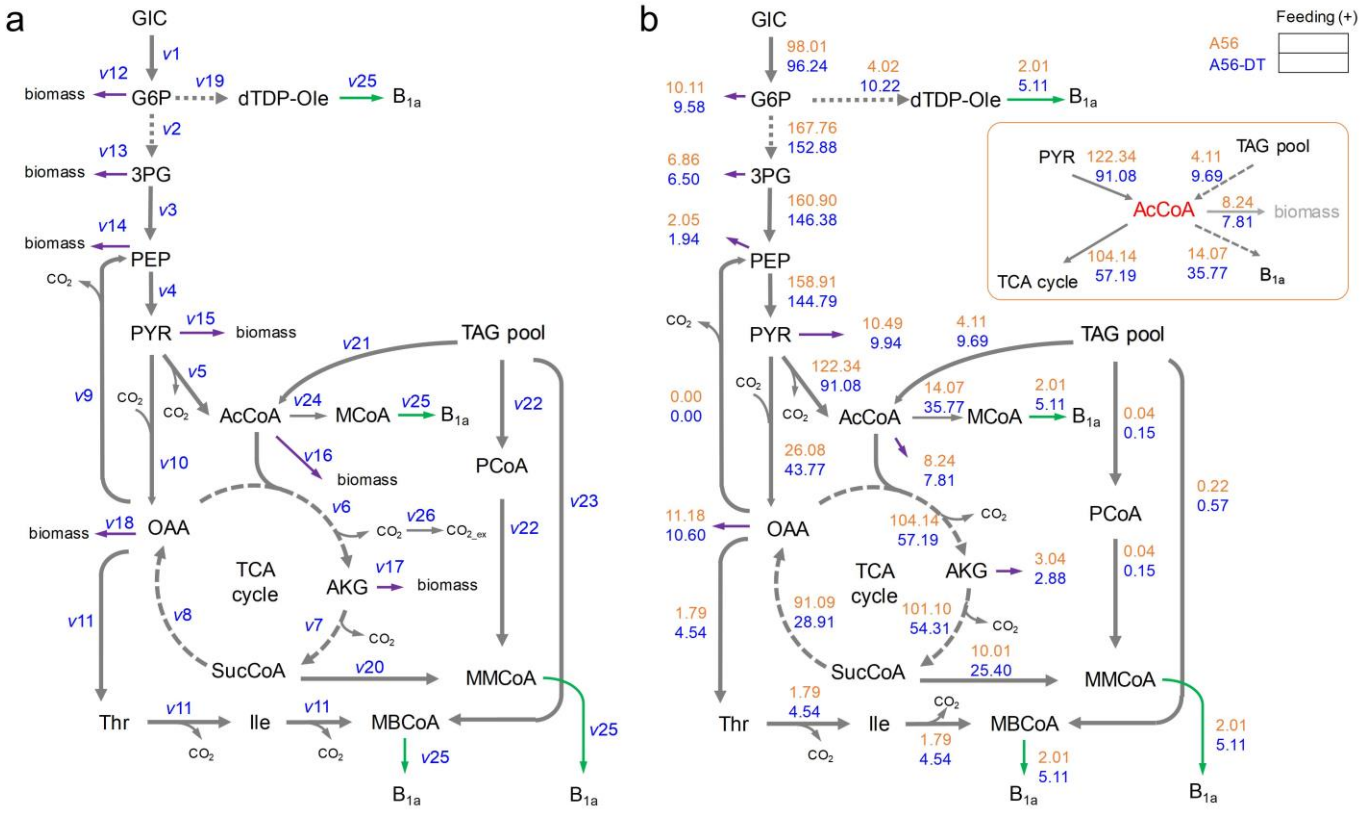

Supplementary Figure 15

Carbon flux distribution of *S. avermitilis* by metabolic flux analysis.

(a) Simplified metabolic network of *S. avermitilis*. Flux for biomass biosynthesis from the G6P node (*v*12) including fluxes from five different precursors (glucose-6-phosphate, fructose-6-phosphate, ribose-5-phosphate, erythrose-4-phosphate, glyceraldehyde-3-phosphate). 15 detected fatty acid moieties from cellular TAGs in *S. avermitilis* were detected, and flux *v*21 represents the sum of specific production rate of AcCoA from degradation of these 15 fatty acids. Similarly, *v*22 and *v*23 represent the sum of specific production rate of PCoA from degradation of two fatty acids (C15:0 and C17:0) and the sum of specific production rate of MBCoA from degradation of three fatty acids (aiC13:0, aiC15:0, and aiC17:0), respectively. The biochemical reactions, stoichiometric equations and experimentally determined fluxes are shown in Supplementary Table 11–13. (b) Actual fluxes of A56 and A56-DT in fed-batch fermentation. The inset showed the mass balance of the AcCoA node, and fluxes were expressed in unit of the acetyl unit. Data for metabolic flux analysis were collected during stationary phase (120–196 h). Data shown here were the average of three independent experiments. Abbreviations: PCoA, propionyl coenzyme A; MCoA, malonyl coenzyme A; MMCoA, methylmalonyl coenzyme A; MBCoA, 2-methylbutyryl coenzyme A; SucCoA, succinyl coenzyme A; dTDP-Ole, deoxythymidine diphosphate-oleandrose; L-Asp, L-aspartate; L-Thr, L-threonine; Ile, L-isoleucine; B_{1a}, avermectin B_{1a}; other abbreviations were shown in Supplementary Fig. 10.

Supplementary Table 1 Optimization of the steps for preparation metabolome samples

Key step[a]	Parameter optimization					
Quenching	Time (min)	2	4	6	8	10
	Metabolite number	272	356	320	202	110
Cell harvest	Approach	Centrifugation		Fast filtration		
	Metabolite number	362		389		
Metabolites extraction	Freezing time (min)	0.75		3		5
	Metabolite number	417		317		286

[a]Unless parameter changed, the conditions for sample preparation were quenching by methanol/water (3:2, v/v) for 4 min, harvesting cells by centrifugation (-15 °C, 12,000 × *g*, 3 min), and freezing the mixture of cell powder and methanol/water (1:1, v/v) in liquid nitrogen for 1 min.

Supplementary Table 2 The identified metabolites in this work

Please see separate file for Supplementary Table 2

Supplementary Table 3 Correlation of fatty acid moieties of cellular TAG pool with glucose consumption and Act production in M145

RT/mz	Fatty acid moieties of TAGs	Correlation coefficient (r)[a]			
		Primary metabolism (20–48 h)	Rank	Polyketide production stage (72–96 h)	Rank
21.672/74	TAG-iC13:0	-0.84848	59	-0.93829	1
21.842/74	TAG-aiC13:0	-0.95722	15	-0.98451	14
23.882/74	TAG-iC14:0	-0.97752	3	-0.97646	5
24.671/74	TAG-C14:0	-0.9634	9	-0.97164	8
26.001/74	TAG-iC15:0	-0.95323	19	-0.98101	2
26.186/74	TAG-aiC15:0	-0.96862	6	-0.97867	4
26.74/74	TAG-C15:0	-0.94184	24	-0.94393	12
28.02/74	TAG-iC16:0	-0.93839	27	-0.9421	13
28.332/74	TAG-C16:1-Δ9	-0.96185	11	-0.97593	6
28.723/74	TAG-C16:0	-0.91709	37	-0.92964	16
29.925/74	TAG-iC17:0	-0.9876	2	-0.9628	9
30.095/74	TAG-aiC17:0	-0.96624	8	-0.97514	7
30.621/74	TAG-C17:0	-0.95603	16	-0.9588	11
31.986/74	TAG-C18:1-Δ9	-0.6568	191	-0.71368	55
32.434/74	TAG-C18:0	-0.94157	25	-0.9798	3

[a]Correlation coefficient here indicates the Pearson correlation coefficient. It indicates the correlation between the variation pattern of a metabolite and that of glucose consumption in primary metabolism, or Act production in late stationary phase, respectively.

Supplementary Table 4 Correlations of fatty acid moieties of cellular TAG pool with glucose consumption and Act production in HY01

RT/mz	Fatty acid moieties of TAGs	Correlation coefficient (r)[a]			
		Primary metabolism (20-48 h)	Rank	Polyketide production stage (72-96 h)	Rank
21.672/74	TAG-iC13:0	-0.7865	63	-0.93736	11
21.842/74	TAG-aiC13:0	-0.84916	89	-0.58173	35
23.882/74	TAG-iC14:0	-0.86833	75	-0.53006	46
24.671/74	TAG-C14:0	-0.91205	35	-0.96277	7
26.001/74	TAG-iC15:0	-0.72376	277	-0.9298	13
26.186/74	TAG-aiC15:0	-0.78207	186	-0.97033	3
26.74/74	TAG-C15:0	-0.95761	65	-0.96166	8
28.02/74	TAG-iC16:0	-0.97729	4	-0.96999	4
28.332/74	TAG-C16:1-Δ9	-0.96103	19	-0.96027	9
28.723/74	TAG-C16:0	-0.9646	55	-0.97716	1
29.925/74	TAG-iC17:0	-0.8161	107	-0.89964	15
30.095/74	TAG-aiC17:0	-0.82096	31	-0.97077	2
30.621/74	TAG-C17:0	-0.81969	142	-0.70801	24
31.986/74	TAG-C18:1-Δ9	-0.29436	604	-0.46438	66
32.434/74	TAG-C18:0	-0.82808	221	-0.89942	16

[a]Correlation coefficient here indicates the Pearson correlation coefficient. It indicates the correlation between the variation pattern of a metabolite and that of glucose consumption in primary metabolism, or Act production in late stationary phase, respectively.

Supplementary Table 5 Transcriptional profiles of genes in fatty acid biosynthesis and *β*-oxidation pathway in M145

Gene[a]	Protein function	18 h	24 h	30 h	36 h	42 h	48 h	60 h
Fatty acid biosynthesis								
*sco*0548	3-oxoacyl-(ACP) synthase	0	-0.040571	0.048164	-0.27023	-0.318568	-0.450826	0.03595
*sco*1271	3-oxoacyl-(ACP) synthase III	0	-1.064465	-0.59611	-1.210535	-0.563451	-0.880529	-0.556887
*sco*1814	enoyl-(ACP) reductase	0	0.664	0.854873	-1.361942	-1.388662	-1.192347	-1.760221
*sco*1815	3-oxacyl-(ACP) reductase	0	0.662662	0.954164	-1.087674	-1.259263	-0.828376	-1.346785
*sco*2387	ACP S-malonyltransferase	0	2.399197	2.820683	1.297573	1.154597	1.148039	0.84856
*sco*2388	3-oxoacyl-(ACP) synthase III	0	2.263427	2.599718	0.656432	0.791094	0.841054	0.247539
*sco*2390	3-oxoacyl-(ACP) synthase II	0	2.822072	3.329178	1.374524	1.511346	1.189047	0.75138
*sco*3246	3-oxoacyl-(ACP) synthase III	0	3.619661	3.386896	2.113213	1.644384	0.903683	-0.2051
*sco*3248	3-oxoacyl-(ACP) synthase II	0	3.893134	3.493597	2.051836	1.405181	0.635099	-0.400131
*sco*6564	3-oxoacyl-(ACP) synthase III	0	2.041764	2.395511	0.786719	-0.026315	-0.054981	-0.28862
Fatty acid degradation (β-oxidation)								
*sco*1690	acyl-CoA dehydrogenase	0	0.435393	0.64804	0.228441	0.387759	0.432775	0.384395
*sco*2774	acyl-CoA dehydrogenase	0	-1.257016	-0.941887	-0.348108	-0.427168	0.631835	1.113566
*sco*3079	acetyl-CoA acetyltransferase	0	-0.428967	-0.327443	0.197453	0.762681	1.52582	1.920303
*sco*6026	fatty acid oxidation complex alpha-subunit	0	0.33732	0.263391	0.155749	0.572081	1.049114	1.733756
*sco*6027	acetyl-CoA acetyltransferase (thiolase)	0	0.700178	0.545147	0.47856	0.710027	1.249628	1.996327
*sco*6731	acetyl-CoA acetyltransferase (thiolase)	0	0.903135	0.882844	0.565504	1.020797	1.809001	2.470262
*sco*6732	fatty acid oxidative multifunctional enzyme	0	1.365282	1.215275	0.909906	1.526041	1.990148	2.708983
*sco*6787	acyl-CoA dehydrogenase	0	0.215089	-0.748402	-0.021894	0.146551	0.126047	0.229735
*sco*6788	acetyl-CoA acetyltransferase	0	0.217677	0.083742	-0.169445	0.059013	0.743502	0.621189

*sco*6789	fatty oxidation protein	0	-0.035315	-0.472083	-0.144739	0.151648	0.347302	0.492704

[a]Data of this time-course transcriptome were deposited in GEO database (No. GSE53562).

Supplementary Table 6 Biochemical reactions used for metabolic flux analysis of *S. coelicolor*

Pathway classification	Flux[a]	Reaction[b,c]
Glycolysis	*v*1	GLC + ATP -> G6P + ADP
	*v*3	G6P + ATP + 2NADP <-> 2 3PG + ADP + 2NADPH
	*v*5	3PG <-> PEP
	*v*7	PEP + ADP -> PYR + ATP
TCA cycle	*v*9	PYR + CoA -> AcCoA + CO_2
	*v*10	AcCoA + OAA + NADP -> CoA + NADPH + AKG + CO_2
	*v*11	AKG + ADP + NAD -> CO_2 + ATP + NADH + OAA
Anaplerotic route	*v*12	OAA + GTP -> PEP + CO_2 + GDP
	*v*16	PYR + ATP + CO_2 -> OAA + ADP
TAG degradation	*v*19	C16:0 + 8CoA + ATP + 7FAD + 7NAD -> 7NADH + 8AcCoA + 7$FADH_2$ + AMP
Act biosynthesis	*v*13	16AcCoA + 16ATP + 6NADPH + 3NAD + 2O_2-> Act + 16 NADP + 3 NADH + 16ADP + 16CoA + 6H_2O
Biomass biosynthesis	*v*2, *v*4, *v*6, *v*8, *v*14, *v*17, *v*18	0.0851G6P + 0.0929F6P + 0.3093R5P + 0.0398E4P + 0.0478G3P + 0.3165-3PG + 0.0854PEP + 0.2290PYR + 1.6540AcCoA + 0.1102AKG + 0.3662OAA + 0.892517.5515ATP + 10.0429NADPH + 0.0005O_2 -> BIOMASS + 0.0631CO_2 + 2.2470NADH

[a]The flux number is in accordance with that shown in Supplementary Fig. 10a.

[b]Degradation of fatty acid moieties of TAGs were used to indicate TAG degradation in this work. Since different fatty acid have the same degradation pattern, we took palmitic acid as an example to show the stoichiometric number of generating acetyl-CoA. There were 15 detected fatty acid moieties of TAGs, and flux *v*19 was used to represent the sum of specific production rate of AcCoA from degradation of these fatty acids. The unit of coefficient in biomass biosynthetic reaction is g/g DCW. Biomass biosynthesis of *S. coelicolor* was described by Coze et al. (PLoS One 8, e84151, 2013).

[c]Abbreviations: F6P, fructose-6-phosphate; R5P, ribose-5-phosphate; E4P, erythrose-4-phosphate; G3P, glyceraldehyde-3-phosphate; ATP, adenosine triphosphate; ADP, adenosine diphosphate; AMP, adenosine monophosphate; NADH, reduced nicotinamide adenine dinucleotide; NAD, oxidized nicotinamide adenine dinucleotide; NADPH, reduced nicotinamide adenine dinucleotide phosphate; NADP, oxidized nicotinamide adenine dinucleotide phosphate; $FADH_2$, reduced flavin adenine dinucleotide; FAD, oxidized flavin adenine dinucleotide. Other abbreviations were shown in Supplementary Fig. 10.

Supplementary Table 7 Stoichiometric equations of metabolic flux analysis for *S. coelicolor*

Number	Equation[a]	Corresponding intermediate
R1	$v1-v2-0.5\times v3=0$	G6P
R2	$v3-v4-v5=0$	3PG
R3	$v5+v12-v6-v7=0$	PEP
R4	$v7-v8-v9-v16=0$	PYR
R5	$v9+v19-v10-v14-16\times v13=0$	AcCoA
R6	$v10-v11-v17=0$	AKG
R7	$v16+v11-v10-v12-v18=0$	OAA
R8	$v9+v10+v11+v12-v15=0$	CO_2

[a]Among all 19 fluxes, 11 fluxes were experimentally determined, including $v1$(glucose uptake rate), $v2$, $v4$, $v6$, $v8$, $v14$, $v17$ and $v18$ (biomass biosynthesis), $v19$ (AcCoA production rate from degradation of 15 fatty acid moieties of TAGs), $v13$ (Act production rate), $v15$ (CO_2 production rate). Data of determined fluxes were listed in Supplementary Table 8.

Supplementary Table 8 Experimentally determined flux for metabolic flux analysis of *S. coelicolor*

Flux[a]	Experimental metabolic flux (μmol/gDCW/h)[b]					Description
	Feeding (-)			Feeding (+)		
	M145	HY01	M145-DT	M145	HY01	
*v*1	12.11	11.21	11.50	108.94	106.71	glucose uptake
*v*2	2.50	2.37	2.44	21.19	21.03	biomass
*v*4	1.70	1.61	1.66	14.37	14.26	biomass
*v*6	0.51	0.48	0.49	4.29	4.26	biomass
*v*8	2.60	2.46	2.53	21.96	21.80	biomass
*v*13	1.14	2.58	2.95	1.46	3.51	Act biosynthesis
*v*14	2.04	1.93	1.99	17.26	17.12	biomass
*v*15	24.48	13.49	12.10	251.16	205.31	CO_2 production
*v*17	0.75	0.71	0.73	6.37	6.32	biomass
*v*18	2.77	2.62	2.70	23.42	23.25	biomass
*v*19	16.62	35.59	40.65	11.73	26.93	TAG degradation

[a]Flux is corresponding to that shown in Supplementary Fig. 10a.

[b]Specific growth rate of M145 and HY01 in batch fermentation are both 0.0010 h^{-1}, and those in fed-batch fermentation are 0.0084 h^{-1} and 0.0083 h^{-1}, respectively. Data shown were the average of three replicates.

Supplementary Table 9 Transcriptional profiles of ACSs in M145

Gene[a]	18 h	24 h	30 h	36 h	42 h	48 h	60 h
*sco*1330	0	0.373017	0.609303	0.595309	0.588651	0.477248	0.230877
*sco*2131	0	-1.33243	-1.13272	-0.84897	-1.13219	-0.46744	0.046373
*sco*2444	0	0.219652	0.200627	-0.16148	0.200257	1.003049	0.101617
*sco*2561	0	-1.08563	-0.99657	-0.94044	-0.73007	-0.26452	0.589498
*sco*2720	0	-0.01777	0.109849	0.013591	-0.26615	0.011752	0.32353
*sco*3436	0	0.07702	-0.44036	-0.62563	-0.38935	-0.24093	-0.03717
*sco*4006	0	1.151524	0.690835	1.41555	2.691003	2.026255	2.406068
*sco*4503	0	-0.65631	-0.29498	-0.24575	-0.24889	-0.38867	-0.10353
*sco*5983	0	-0.50172	-0.87788	-0.59888	-0.11977	-0.45727	-0.30702
*sco*6196	0	-0.02513	-0.08791	-0.02418	0.073659	0.156673	-0.79279
*sco*6552	0	-0.50441	-0.48455	-0.29585	-0.80583	-0.54177	-0.40387
*sco*6790	0	0.155172	0.242353	0.572804	0.702958	0.304657	0.320831
*sco*6968	0	0.717845	0.768942	0.2589	0.616592	-0.08325	0.700291
*sco*7244	0	-0.03603	-0.11276	0.109055	1.110657	0.955282	0.645736
*sco*7329	0	1.403925	1.33705	1.344174	1.167211	0.991301	0.57347
*sco*4383	0	-0.54136	-0.37794	-0.09921	-0.04646	0.115752	-0.2211

[a]Data of this time-course transcriptome were deposited in GEO database (No. GSE53562). Genes were first selected according to KEGG database, and further adding genes annotated as acyl-CoA synthetase or long chain fatty acid CoA ligase, as well as genes with high similarities with FadD of *E. coli* identified by blasting.

Supplementary Table 10 Details of 888 ACSs

Please see separate file for Supplementary Table 10

Supplementary Table 11 Biochemical reactions used for metabolic flux analysis of *S. avermitilis*

Pathway classification	Flux[a]	Reaction[b,c]
Glycolysis	*v*1	GLC + ATP -> G6P + ADP
	*v*2	G6P + ATP + 2NADP <-> 2 3PG + ADP + 2NADPH
	*v*3	3PG <-> PEP
	*v*4	PEP + ADP -> PYR + ATP
TCA cycle	*v*5	PYR + CoA -> AcCoA + CO_2
	*v*6	AcCoA + OAA + NADP -> CoA + NADPH + AKG + CO_2
	*v*7	AKG + CoA + NAD -> SucCoA + CO_2 + NADH
	*v*8	SucCoA + GDP + FAD + NAD -> OAA + $FADH_2$ + NADH + GTP + CoA
Anaplerotic route	*v*9	OAA + GTP -> PEP + CO_2 + GDP
	*v*10	PYR + ATP + CO_2 -> OAA + ADP
TAG degradation	*v*21	C16:0 + 8CoA + ATP + 7FAD + 7NAD -> 7NADH + 8AcCoA + $7FADH_2$ + AMP
	*v*22	C15:0 + 7CoA + ATP + 6FAD + 6NAD -> 6NADH + 6AcCoA + PCoA + $6FADH_2$ + AMP
	*v*23	aiC13:0 + 5CoA + ATP + 4FAD + 4NAD -> 4NADH + 4AcCoA + MBCoA + $4FADH_2$ + AMP
Precursor biosynthesis	*v*11	OAA + NH_3 + NADPH -> L-Asp + NADP
	*v*11	L-Asp + 2ATP + 2NADPH -> L-Thr + 2ADP + 2NADP
	*v*11	L-Thr + PYR + 2NADPH + Glu -> NH_3 + CO_2 + Ile + AKG + 2NADP
	*v*11	Ile + AKG + NAD + CoA -> MBCoA + NADH + CO_2 + Glu
	*v*20	SucCoA -> MMCoA

	*v*22	PCoA + CO_2 -> MMCoA
	*v*24	AcCoA + CO_2 -> MCoA
	*v*19	G6P + dTTP -> dTDP-Ole + PPi
B_{1a} biosynthesis	*v*25	2dTDP-Ole + MBCoA + 7MCoA + 5MMCoA + O_2 + 9NAPDH -> B1a + 12CO_2 + 9NADP + 13CoA
Biomass biosynthesis	*v*12-*v*18	0.0851G6P + 0.0929F6P + 0.3093R5P + 0.0398E4P + 0.0478G3P + 0.3165-3PG + 0.0854PEP + 0.2290PYR + 1.6540AcCoA + 0.1102AKG + 0.3662OAA + 0.892517.5515ATP + 10.0429NADPH + 0.0005O_2 -> BIOMASS + 0.0631CO_2 + 2.2470NADH

[a]The flux number is in accordance with that shown in Supplementary Fig. 15a.

[b]C16:0, C15:0, and aiC13:0 were chosen as examples to show the stoichiometric number of generating AcCoA, PCoA, and MBCoA, respectively. Flux *v*21, *v*22, and *v*23 represent the sum of specific production rate of AcCoA, PCoA, and MBCoA from degradation of corresponding fatty acid moieties of TAGs, respectively. Details were described in legend of Supplementary Fig. 15. The unit of coefficient in biomass biosynthetic reaction is g/g DCW. Biomass biosynthesis of *S. avermitilis* was referred to that of *S. coelicolor*.

[c]Abbreviations were shown in Supplementary Fig. 10 and 15, and Supplementary Table 6.

Supplementary Table 12 Stoichiometric equations of metabolic flux analysis for *S. avermitilis*

Number	Equation[a]	Metabolite
R1	$v1-v12-v19-0.5\times v2=0$	G6P
R2	$v19-2\times v25=0$	dTDP-Ole
R3	$v2-v13-v3=0$	3PG
R4	$v3+v9-v4-v14=0$	PEP
R5	$v4-v5-v10-v15=0$	PYR
R6	$v5+v21-v6-v16-v24=0$	AcCoA
R7	$v24-7\times v25=0$	MCoA
R8	$v6-v7-v17=0$	AKG
R9	$v7-v8-v20=0$	SucCoA
R10	$v8+v10-v9-v11-v18-v6=0$	OAA
R11	$v11+v23-v25=0$	MBCoA
R12	$v20+v22-5\times v25=0$	MMCoA
R13	$v5+v6+v7+v9+2\times v11-v26=0$	CO_2

[a]Among all 26 fluxes, 13 fluxes were experimentally determined, including $v1$(glucose uptake rate), $v12$ to $v18$ (biomass biosynthesis), $v21$-$v23$ (AcCoA, PCoA, and MBCoA production rate from degradation of corresponding fatty acid moieties of TAGs), $v25$ (B_{1a} production rate), $v26$ (CO_2 production rate). Data of determined fluxes were listed in Supplementary Table 13.

Supplementary Table 13 Experimentally determined flux for metabolic flux analysis of *S. avermitilis*

Flux[a]	Experimental determined metabolic flux (μmol/gDCW/h)[b]		Description
	A56	A56-DT	
*v*1	98.01	96.24	glucose uptake
*v*12	10.11	9.58	biomass
*v*13	6.86	6.50	biomass
*v*14	2.05	1.94	biomass
*v*15	10.49	9.94	biomass
*v*16	8.24	7.81	biomass
*v*17	3.04	2.88	biomass
*v*18	11.18	10.60	biomass
*v*21	4.11	9.69	TAG degradation
*v*22	0.04	0.15	TAG degradation
*v*23	0.22	0.57	TAG degradation
*v*25	2.01	5.11	B_{1a} production
*v*26	331.22	212.01	CO_2 production

[a]Flux is corresponding to that shown in Supplementary Fig. 15a.

[b]Data were obtained from fed-batch fermentation during 120 h to 192 h. Specific growth rate of A56 and A56-DT are 0.0040 h^{-1} and 0.0038 h^{-1}, respectively. Data shown were the average of three replicates.

Supplementary Table 14 Primers used in this work

Primer		Sequence (5'-3')
Usage	Name	
Construction of pCu-SCO6196	CuF	aagcttgggctgcaggtcgactctagagttatcaccgcttgaacttggc
	CuR	gacggctggggcgcgggtgcggtcactggggtcctcctgttgctcgactagtataatac
	6196F	gtgaccgcacccgcgccccagccgtc
	6196R	acatgattacgaattcgatatcgcgcgcggccgcggatctcaggggcgcgctccgtacc
Confirmation of pCu-SCO6196	LCF	gccaagttcaagcggtgataatctagacgctccctgcccgctatggtgacga
	LCR	ccctgatgataagcattacgatatcgaattcgtaatcatgtcatagctg
Construction of 6196DM	96LF	cagtgccaagcttgggctgcaggagaacggtccggcgattgtcctcg
	96LR	cgagtgggtcctcgtccagtacgggatccaggagttcctgtacgcccacc
	96RF	tcctggatcccgtactggacgaggacccactcg
	96RR	ctatgacatgattacgaattcgatatcgatgaaactgcgcgcggtcgtc
	1132F	catcgatatcgaattcgtaatcatgtcatag
	1132R	gttctcctgcagcccaagcttggcactggc
Confirmation of 6196DM	96vF	agtaggcgcgcagttcctccag
	96vR	tcccgtccggacggcgctggacctacg
Construction of 6196OE	96F1	atctagcggaacggatctagagatgtgaccgcacccgcgccccagccgtc
	96R1	ttccatcgccgcttcatgatgaattctcgccgcggccgataccggtgc
Construction of pET-SCO6196	96F2	gtgctcgagtgcggccgcaagctttcattaatgatgatgatgatgatgcggacgcgcgccataacgctcac

	96R2	taactttaagaaggagatatacatatgacagcacccgctccacaaccctc
RT-qPCR for *sco*6196	96F2	ggcatctgggcggtcaact
	96R2	gctgctcttgtgggcgagg
RT-qPCR for reference	0710F	tgtccgccctccgctccgtgtcc
	0710R	tccaggaccgtgtcgccgtag
RT-qPCR for *sco*7244	7244F	gtgcagctcctgtacacctc
	7244R	ctcaggtactcgtgcaccag
RT-qPCR for *sco*6968	6968F	cagaccgtctccctcaactc
	6968R	cctccttcaccatcagctcg
RT-qPCR for *sco*4383	4383F	catccagaaccaccgcatca
	4383R	tcagcgaggagaggtcgtag
RT-qPCR for *sco*2444	2444F	agagcggcggttacaagatc
	2444R	cacgatccgttccccgag

Supplementary Notes

Supplementary Note 1

Experimental procedure for metabolome sample preparation of *S. coelicolor* for GC-MS analysis. Detailed procedures are modified based on that described by Lisec et al. (Nat. Protoc. 1, 387-396, 2006). Step 1: Cells were quickly harvested by fast filtration (cellulose acetate membrane (0.8 μm pore size), filter time < 30 s) and washed with 30 ml deionized water (prechilled to 0 °C); Step 2: The harvested cells were quickly transferred into a mortar and submerged in liquid nitrogen (30 s) for quenching. The frozen cells could be stored at -80 °C for a few weeks if the following steps are not processed immediately. Step 3: The frozen cells were ground into powder in liquid nitrogen. Step 4: Cell powder (200 mg) was quickly suspended with 1.0 ml prechilled (-20 °C) extraction buffer of 50% (v/v) methanol/water and vortexed in cold ethanol bath (-20 °C) for 30 s. The mixture was then subjected to three freeze-thaw cycles (45 s/3 min, respectively). After centrifugation (-15 °C, 13,000 × g, 10 min), the supernatant (0.8 ml) was collected and the pellets were re-extracted twice by the addition of 0.5 ml extraction buffer and the extracts were combined. To the total of 1.3 ml of metabolite extract was added 100 μl of d_4-succinic acid (0.14 mg/ml) as the internal standard to correct minor variations. Step 5: The extraction was frozen and lyophilized by a vacuum concentrator overnight. Step 6: Methoxamine hydrochloride was dissolved in pyridine at a concentration of 20 mg/ml for immediate use (Anal. Chem. 80, 2939-2948, 2008). For each sample, 60 μl methoxamine hydrochloride was added and incubated in a water bath at 40 °C for 90 min. Samples were vortexed for 30 s every 15 min of the incubation period. Step 7: N-methyl-N-(trimethylsilyl)-trifluoroacetamide (MSTFA) (80 μl) was added and incubated under the same condition as in step 6. Step 8: Samples were centrifuged at 13,000 × g for 10 min and analyzed by GC-MS within 24 h.

Supplementary Note 2

Composition of integrated metabolome. The integrated metabolome data are composed of a total of 796 metabolites from six timepoint (five independent experimental replicates for each timepoint). The 796 metabolites include 776 general metabolites obtained by GC-MS with our improved method (Supplementary Note 1), 16 fatty acid moieties of TAGs quantified by GC-MS, acetyl-CoA and malonyl-CoA quantified by LC-MS/MS, as well as glucose and actinorhodin.

Supplementary Note 3

Structure of actinorhodin-related metabolites. To trace the ^{13}C labeled carbon flux towards actinorhodin, we analyzed five different actinorhodin-related compounds by LC-MS/MS, including γ-actinorhodin (Molecular Weight: 630.51), γ'-actinorhodin (Molecular Weight: 632.53), actinorhodin (Molecular Weight: 634.55), unknown

actinorhodin (Molecular Weight: 646.51), ε-actinorhodin (Molecular Weight: 648.53) (J. Bacteriol. 178, 2238-2244, 1996).

Supplementary Note 4

Python scripts for flux sampling analysis.

```
# this code is used to conduct flux sampling analysis for Streptomyces
# started
from __future__ import print_function
import os
# for the sampling analysis, You have uncovered a small bug :) Until it's fixed, please
#downgrade to cobra 0.14.2 and remove the line referencing model._sbml
from cobra.io import read_sbml_model
from cobra.flux_analysis import pfba
from cobra.sampling.optgp import OptGPSampler
import pprint
import sys
import pandas as pd
from cobra import Model, Reaction, Metabolite



os.chdir('/Users/luho/PycharmProjects/model/cobrapy/code')
sys.path.append(r"/Users/luho/PycharmProjects/model/cobrapy/code")
pprint.pprint(sys.path)

# import self function
from mainFunction import *
# test for the GEM_new
GEM_new = read_sbml_model('../data/iKS1317.xml')
model1 = GEM_new.copy()
model = model1



# firstly check the cell growth
# flux calculation under reference condition
model.reactions.get_by_id("EX_glc__D_e").bounds = (-12.11,-12.11) #glu
model.reactions.get_by_id("EX_co2_e").bounds = (24.48,24.48) #co2
# optimize
model.objective = 'BIOMASS_SCO'
pfba_solution = pfba(model)
flux1 = pd.DataFrame(pfba_solution.fluxes)
flux1.index.name = 'rxnID'
flux1.reset_index(inplace=True)
# check the exchange rates
```

```
flux_exchange = flux1[flux1['rxnID'].str.contains('EX_')]
pfba_solution.fluxes['BIOMASS_SCO']

'''
# sampling
# GLPK is good there since it has faster basis recycling than Gurobi or Cplex.
gr = pfba_solution.fluxes['BIOMASS_SCO']
co = model.problem.Constraint(model.reactions.r_4041.flux_expression,
lb=0.95*(gr))
model.add_cons_vars([co])
optgp = OptGPSampler(model, processes = 8)
s = optgp.sample(1000)
'''


# just for the analysis
# here we fist fix the biomass and maximize the production
model = read_sbml_model('../data/iKS1317.xml')
# Add the reactions for TAG degrade
model.add_metabolites(Metabolite('tag160_e'))
# TAG degradation
dict1 = {model.metabolites.get_by_id('tag160_c'): -1,
            model.metabolites.get_by_id('coa_c'): -24,
            model.metabolites.get_by_id('atp_c'): -3,
            model.metabolites.get_by_id('fad_c'): -21,
            model.metabolites.get_by_id('nad_c'): -21,
            model.metabolites.get_by_id('h2o_c'): -21,
            model.metabolites.get_by_id('nadh_c'):21,
            model.metabolites.get_by_id('accoa_c'):24,
            model.metabolites.get_by_id('fadh2_c'):21,
            model.metabolites.get_by_id('glyc_c'):1,
            model.metabolites.get_by_id('amp_c'):3,
            model.metabolites.get_by_id('ppi_c'):3,
            model.metabolites.get_by_id('h_c'):24
            }

# using the general procedures to add the new function
reaction = Reaction('TAG_degrade')
reaction.name = 'TAG_degradation'
reaction.subsystem = 'new added'
reaction.lower_bound = 0.    # This is the default
reaction.upper_bound = 1000.    # This is the default
reaction.EC = ''
reaction.add_metabolites(dict1)
```

```
reaction.gene_reaction_rule = ''
model.add_reactions([reaction])

# transport
dict2 = {model.metabolites.get_by_id('tag160_e'): -1,
         model.metabolites.get_by_id('tag160_c'):1,
         }
reaction = Reaction('TAG_transport')
reaction.name = 'TAG_transport'
reaction.subsystem = 'new added'
reaction.lower_bound = 0.    # This is the default
reaction.upper_bound = 1000.    # This is the default
reaction.EC = ''
reaction.add_metabolites(dict2)
reaction.gene_reaction_rule = ''
model.add_reactions([reaction])

# exchange
dict3 = {model.metabolites.get_by_id('tag160_e'): -1
         }
reaction = Reaction('TAG_exchange')
reaction.name = 'TAG_exchange'
reaction.subsystem = 'new added'
reaction.lower_bound = -1000.    # This is the default
reaction.upper_bound = 0.    # This is the default
reaction.EC = ''
reaction.add_metabolites(dict3)
reaction.gene_reaction_rule = ''
model.add_reactions([reaction])
# check the added reactions
for r in model.reactions:
    print(r.id, r.name, r.reaction, r.compartments, sep="\t")


# with glucose uptake as objective function
# calculation
#M145 no feeding as an example
with model:
    model.reactions.get_by_id("EX_glc__D_e").bounds = (-1000, 0)    # glu
    model.reactions.get_by_id("TAG_exchange").bounds = (-0.676, -0.676)    # fix
TAG
    model.reactions.get_by_id('BIOMASS_SCO').bounds = (1, 1)
    model.reactions.get_by_id("EX_co2_e").bounds = (24.48, 24.48)    # co2
    model.reactions.get_by_id("DM_ACT_c").bounds = (1.1425, 1.1425)
```

```
        #model.objective = 'DM_ACT_c'
        model.objective = 'EX_glc__D_e'
        pfba_solution = pfba(model)
        #print('act:', pfba_solution.fluxes['DM_ACT_c'])
        print('glc:', pfba_solution.fluxes['EX_glc__D_e'])
        #flux sampling
        gr1 = pfba_solution.fluxes['EX_glc__D_e']
        co = model.problem.Constraint(model.reactions.EX_glc__D_e.flux_expression,
lb=1.02 * (gr1))
        model.add_cons_vars([co])
        optgp = OptGPSampler(model, processes=8)
        s1 = optgp.sample(1000)
```